

# An improved cosmological model fitting of Planck data with a dark energy spike

Chan-Gyung Park

*Division of Science Education and Institute of Fusion Science,  
Chonbuk National University, Jeonju 561-756, Republic of Korea*

(Dated: March 5, 2015)

The  $\Lambda$  cold dark matter ( $\Lambda$ CDM) model is currently known as the simplest cosmology model that best describes observations with minimal number of parameters. Here we introduce a cosmology model that is preferred over the conventional  $\Lambda$ CDM one by constructing dark energy as the sum of the cosmological constant  $\Lambda$  and the additional fluid that is designed to have an extremely short transient spike in energy density during the radiation-matter equality era and the early scaling behavior with radiation and matter densities. The density parameter of the additional fluid is defined as a Gaussian function plus a constant in logarithmic scale-factor space. Searching for the best-fit cosmological parameters in the presence of such a dark energy spike gives a far smaller chi-square value by about five times the number of additional parameters introduced and narrower constraints on matter density and Hubble constant compared with the best-fit  $\Lambda$ CDM model. The significant improvement in reducing chi-square mainly comes from the better fitting of Planck temperature power spectrum around the third ( $\ell \approx 800$ ) and sixth ( $\ell \approx 1800$ ) acoustic peaks. The likelihood ratio test and the Akaike information criterion suggest that the model of dark energy spike is strongly favored by the current cosmological observations over the conventional  $\Lambda$ CDM model. However, based on the Bayesian information criterion which penalizes models with more parameters, the strong evidence supporting the presence of dark energy spike disappears. Our result emphasizes that the alternative cosmological parameter estimation with even better fitting of the same observational data is allowed in the Einstein's gravity.

PACS numbers: 98.80.-k, 95.36.+x

## I. INTRODUCTION

It is one of the primary aims in cosmology to find the simplest model that best describes the astronomical observations. Until now, the best concordance model with minimal number of parameters is currently known as the  $\Lambda$  cold dark matter ( $\Lambda$ CDM) model with the cosmological constant  $\Lambda$  as dark energy and CDM as dominant dark matter [1–3].

Many efforts have been made to develop a cosmology model that is better than the conventional  $\Lambda$ CDM model. Determining which model is preferred over the other is a problem of model selection. The standard approach used in the model selection is that one constrains the new model with data using the likelihood method and checks whether or not it is supported over the previous best model based on the statistical criteria. In usual cases, the new candidate cosmology model has more free parameters than  $\Lambda$ CDM model while it often gives a better fitting of observational data. However, simply adding more parameters and getting smaller chi-square (or larger likelihood) does not make the relevant model rank as a better model. In order for a new cosmology model to be ranked as a model better than  $\Lambda$ CDM model, it should pass through at least one of the model selection criteria such as the likelihood ratio test [4], Akaike information criterion [5], Bayesian information criterion [6], Bayesian evidence, and so on (see also [7–12] for applications in cosmology with brief reviews).

Although many dark energy models have been proposed, most of them give only a small improvement in fitting the observational data compared with the  $\Lambda$ CDM

model and do not pass through the model selection criteria with high significance, implying that the  $\Lambda$ CDM model is the final winner in the competition of model selection [10–21].

Recently, Park et al. [22] investigated the observational effect of the early episodically dominating dark energy based on the minimally coupled scalar field with the Albrecht-Skordis potential, where the dark energy density transiently becomes strong during a short period of time. They show that the presence of the early episodic dark energy can affect the cosmological parameter estimation significantly and conclude that the recent Planck data strongly favor the  $\Lambda$ CDM model because only a limited amount of dark energy with episodic nature is allowed. In this paper, we introduce a fluid version of early transiently dominating dark energy model with the similar episodic nature. Our dark energy model is designed to have a transient spike in energy density during an extremely short period and the early scaling behavior with radiation and matter density. We show that our dark energy model gives a significant improved fit to the recent observational data with different parameter constraints and thus is preferred over the best-fit  $\Lambda$ CDM model based on some model selection criteria. Through the example of dark energy spike model, we show that the alternative parameter estimation with even better fitting of the same observational data is allowed in the Einstein's gravity.

This paper is organized as follows. Sec. II describes the fluid-based dark energy spike model with a transient variation in dark energy density and presents numerical calculations of background evolution of this model. In

Sec. III, observational effects of the dark energy spike are investigated using the recent observational data such as the cosmic microwave background radiation (CMB) data from the Planck satellite and the baryonic acoustic oscillation (BAO) data from the large-scale structure surveys. The cosmological parameters constrained with observations are compared in the presence of or without the dark energy spike. In Sec. IV, we compare our dark energy model with the conventional  $\Lambda$ CDM model based on some statistical criteria used in model selection. The discussion and conclusion are presented in Sec. V. Throughout this paper, we set  $c \equiv 1$  and  $8\pi G \equiv 1$ .

## II. A FLUID-BASED DARK ENERGY SPIKE MODEL

The quintessence-based early episodically dominating dark energy model proposed in [22] is on a solid theoretical footing, but has its limitations. First, it is not easy to control the onset, strength, and duration of the transient dark energy because the behavior of dark energy strongly depends on potential parameters and initial conditions. Second, the scalar-field based dark energy model theoretically does not accommodate the crossing of phantom divide ( $w = -1$ ) in the dark energy equation of state, and thus it is not allowed to consider a *spike*, a transient and abrupt variation of dark energy density, which inevitably induces  $w = -1$  crossing. Here we introduce a fluid model of early dark energy that allows a dark energy spike and is easy to handle numerically.

In the conventional  $\Lambda$ CDM model, we add a new fluid (denoted as  $x$ ) with a transient spike in energy density. We assume that the dark energy density parameter ( $\Omega_x$ ) is represented as the sum of a Gaussian function and a constant in logarithmic scale-factor space,

$$\Omega_x(a) = \frac{\mu_x}{3H^2} = A \exp \left[ -\frac{(\ln a - \ln a_c)^2}{2\sigma^2} \right] + B, \quad (1)$$

where  $\mu_x$  is the energy density of the additional fluid,  $a(t)$  is the cosmic scale factor normalized to unity at present,  $H = \dot{a}/a$  is the Hubble parameter at epoch  $a$  with a dot as a time-derivative, and  $A$ ,  $a_c$ , and  $\sigma$  are interpreted as amplitude (strength), temporal position, and duration of the dark energy spike, respectively. The constant term  $B$  denotes the level of early dark energy that exists from the beginning of the universe and is responsible for the scaling evolution where the dark energy density follows that of the dominant fluid. In this paper, we incorporate the  $x$ -fluid and the cosmological constant  $\Lambda$  into the effective fluid of dark energy (DE). The behavior of dark energy in our model shows early scaling evolution with radiation and matter densities with a sudden dark energy spike at a particular epoch and the late-time acceleration phase due to the cosmological constant. From here on, we call the dark energy model with both scaling and transient behaviors as spike-DE model, and the model only with the scaling behavior as scaling-DE model. Note that both

the  $\Lambda$ CDM model ( $A = 0$ ,  $B = 0$ ) and the scaling-DE model ( $A = 0$  and  $B \geq 0$ ) are nested within the spike-DE model.

In the presence of the  $x$ -fluid, the squared Hubble parameter normalized with the present value is given by

$$\left( \frac{H}{H_0} \right)^2 = \frac{\Omega_{r0}a^{-4} + \Omega_{m0}a^{-3} + \Omega_{\Lambda0} + \Omega_{K0}a^{-2}}{1 - \Omega_x(a)}, \quad (2)$$

where the subindices  $r$ ,  $m$ ,  $K$  represent the radiation, matter, and spatial curvature, respectively, and the subindex zero indicates the present value. We assume that the  $x$ -fluid satisfies the continuity equation,  $\dot{\mu}_x = -3H(\mu_x + p_x)$ . The pressure of the  $x$ -fluid is given by

$$p_x = 3H^2\Omega_x \left( -1 - \frac{2\dot{H}}{3H^2} - \frac{\Omega'_x}{3\Omega_x} \right), \quad (3)$$

where

$$\Omega'_x(a) = \frac{d\Omega_x}{d \ln a} = -\frac{\ln a - \ln a_c}{\sigma^2}(\Omega_x - B) \quad (4)$$

and

$$\begin{aligned} \frac{\dot{H}}{H^2} = \frac{1}{1 - \Omega_x} \left\{ \left( -2\Omega_{r0}a^{-4} - \frac{3}{2}\Omega_{m0}a^{-3} - \Omega_{K0}a^{-2} \right) \right. \\ \left. \times \left( \frac{H_0}{H} \right)^2 + \frac{1}{2}\Omega'_x \right\}. \end{aligned} \quad (5)$$

Throughout this paper, we consider the spatially flat universe ( $\Omega_{K0} = 0$ ). The equation of state of the effective dark energy fluid (denoted with a subindex  $d$ ) becomes

$$w = \frac{p_d}{\mu_d} = -1 - \frac{2\dot{H}\Omega_x}{3H^2(\Omega_x + \Omega_\Lambda)} - \frac{\Omega'_x}{3(\Omega_x + \Omega_\Lambda)}, \quad (6)$$

where  $\mu_d = \mu_x + \Lambda$ ,  $p_d = p_x - \Lambda$ , and  $\Omega_\Lambda = \Lambda/(3H^2)$ . The dark energy density parameter ( $\Omega_d = \Omega_x + \Omega_\Lambda$ ) has three asymptotic values:  $\Omega_d \simeq A + B$  at the onset of the dark energy spike ( $a = a_c$ ),  $\Omega_d \simeq B$  before and after the onset ( $|a - a_c| \gg 0$ ) and before the late-time acceleration ( $a \ll a_0$ ), and  $\Omega_d \simeq B + \Omega_\Lambda$  during the acceleration phase ( $a \approx a_0 \gg a_c$ ).

Figure 1 shows the evolution of density parameters, energy densities, dark energy equation of state, and Hubble parameter in the spike-DE model where a strong dark energy spike occurs at  $a = 10^{-3.5}$  ( $\ln a_c = -8.059$ ), together with those in scaling-DE and  $\Lambda$ CDM models. As expected, the dark energy densities of spike-DE (green) and scaling-DE (grey) models show scaling behaviors following radiation and matter sequentially. The model parameters have been adopted as the best-fit ones obtained with the recent observational data (see Sec. III for details). In the spike-DE model, the dark energy equation of state experiences a change of about three

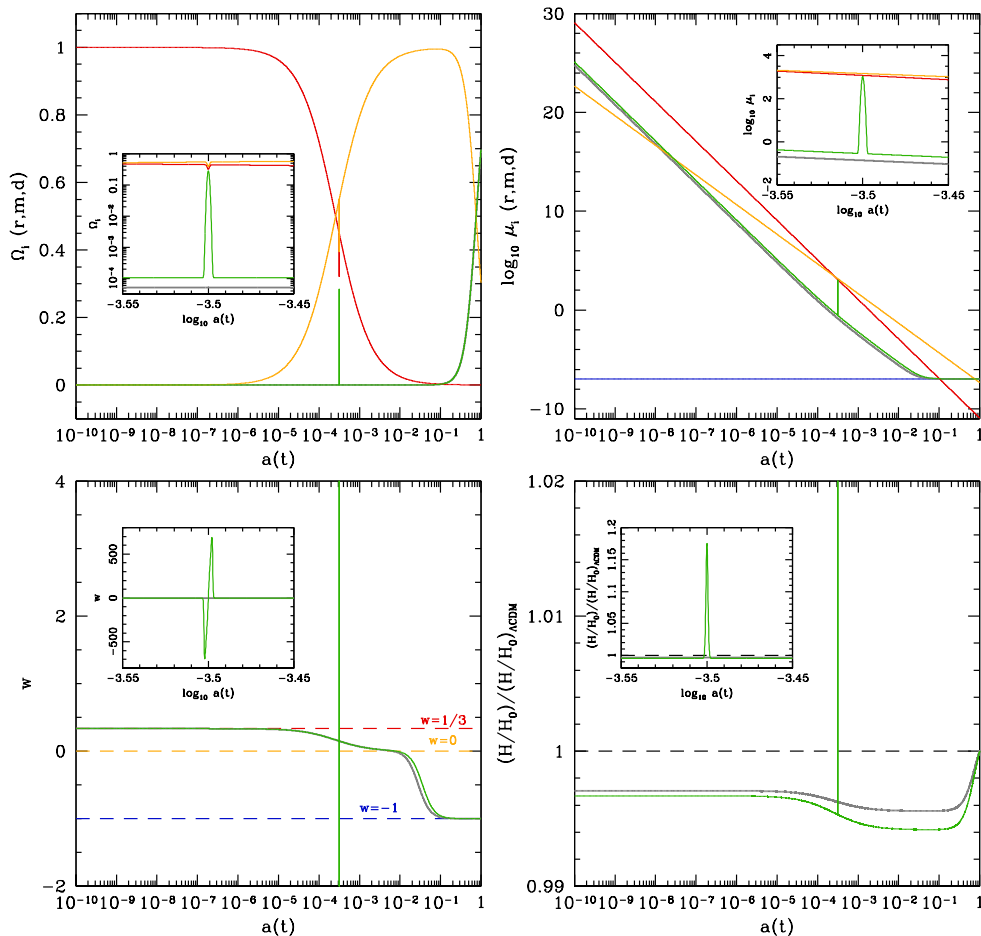


FIG. 1: Evolution of density parameters ( $\Omega_i$ ;  $i = r, m, d$ ), energy densities ( $\mu_i$ ), dark energy equation-of-state ( $w$ ), and normalized Hubble parameter divided by the  $\Lambda$ CDM prediction  $[(H/H_0)/(H/H_0)_{\Lambda\text{CDM}}]$  in the best-fit spike-DE model with  $\log_{10} a_c = -3.5$ ,  $A = 0.28$ ,  $B = 1.1 \times 10^{-4}$ ,  $\sigma = 1.5 \times 10^{-3}$ . In the top-panels, the behaviors of radiation ( $r$ ), matter ( $m$ ), and dark energy ( $d$ ) components are shown as red, yellow, and green curves, respectively. The energy density due to the cosmological constant in the best-fit  $\Lambda$ CDM model is shown as a blue curve (top-right panel). In all panels, grey curves represent the results of scaling-DE model with  $B = 5.2 \times 10^{-5}$ . The precise values of model parameters used in the numerical calculation are presented in Table I.

orders of magnitude with the crossing of phantom divide twice during the occurrence of dark energy spike. Considering 95.4% ( $2\sigma$ ) confidence limits of the Gaussian shape of the spike, it lasts for about 600 years ( $3.153 \times 10^{-4} < a < 3.172 \times 10^{-4}$ ).

### III. OBSERVATIONAL CONSTRAINTS ON THE DARK ENERGY SPIKE MODEL

We probe the observational signatures of our spike-DE model by considering both the scalar- and tensor-type perturbations in a system of multiple components for radiation, matter, and effective dark energy fluid (the  $x$ -fluid plus the cosmological constant). For this aim, we have modified the publicly available CAMB/CosmoMC package (version of Dec. 13 2013) [23, 24] to include the evolution of background and perturbation of the effec-

tive dark energy fluid, and explored the allowed ranges of the conventional cosmological parameters in the presence of a dark energy spike using the Planck CMB data together with other external data sets. For the evolution of perturbed density and velocity of the  $x$ -fluid, the parametrized post-Friedmann prescription for the dark energy perturbations is used to allow the multiple crossing of phantom divide ( $w = -1$ ) in the time-dependent dark energy equation of state [25]. Following the Planck team's analysis, we assume the current CMB temperature as  $T_0 = 2.7255$  K and the effective number of neutrinos as  $N_\nu = 3.046$  with a single massive eigenstate of mass  $m_\nu = 0.06$  eV [2].

We use the CMB data obtained with Planck [37], which is a combination of the CMB temperature anisotropy angular power spectrum up to small angular scales ( $\ell = 2500$ ) and the Wilkinson Microwave Anisotropy Probe 9-year polarization data [26]. We used four Planck CMB

TABLE I: Best-fit cosmological parameters of the spatially flat  $\Lambda$ CDM, scaling-DE, and spike-DE models.

Parameter	$\Lambda$ CDM	Scaling-DE	Spike-DE
$A$	0	0	0.28360
$B$	0	$5.1736 \times 10^{-5}$	$1.0662 \times 10^{-4}$
$\log_{10} a_c$	...	...	-3.5
$\sigma$	...	...	$1.4604 \times 10^{-3}$
$100\Omega_b h^2$	2.21632	2.22226	2.19523
$\Omega_c h^2$	0.11827	0.11778	0.11777
$h$	0.67929	0.68130	0.68158
$\tau$	0.09623	0.08908	0.08873
$n_s$	0.96550	0.96487	0.97147
$r$	0.00048	0.00046	0.01640
$\ln[10^{10} A_s]$	3.09985	3.08397	3.08691
$t_0$ (Gyr)	13.7992	13.7930	13.7983
$A_{100}^{\text{PS}}$	178.3636	138.0731	140.2106
$A_{143}^{\text{PS}}$	62.92783	50.31658	61.88821
$A_{217}^{\text{PS}}$	118.6188	115.4876	126.9649
$A_{143}^{\text{CIB}}$	6.620212	3.852115	5.640900
$A_{217}^{\text{CIB}}$	25.52911	26.94230	23.30611
$A_{143}^{\text{tSZ}}$	3.724382	8.408760	2.995350
$r_{143 \times 217}^{\text{PS}}$	0.9075909	0.8956619	0.9206412
$r_{143 \times 217}^{\text{CIB}}$	0.2190109	0.3866272	$9.2171337 \times 10^{-3}$
$\gamma^{\text{CIB}}$	0.5448702	0.5265283	0.5609424
$c_{100}$	1.000590	1.000599	1.000575
$c_{217}$	0.9963431	0.9962796	0.9968735
$\xi^{\text{tSZ-CIB}}$	0.5315524	$5.734012 \times 10^{-4}$	0.2737207
$A^{\text{ksZ}}$	0.1122116	0.2684244	0.1527581
$\beta_1^1$	0.5376251	0.5772729	0.2189442

likelihood data sets (version of 2013), **Lowlike** for low  $\ell$  temperature and polarization likelihood covering  $\ell = 2$ –32, **Commander** for low  $\ell$  temperature-only likelihood covering  $\ell = 2$ –49, **CamSpec** for high  $\ell$  temperature-only likelihood with  $\ell = 50$ –2500 [27], and **Lensing** for lensing effect [28]. As the external data derived from the large-scale structure observations, we also have used the BAO data points measured by Sloan Digital Sky Survey Data Release 7 (DR7) [29], Baryon Oscillation Spectroscopic Survey Data Release 9 (DR9) [31], 6dF Galaxy Survey [30], and Wiggle Z surveys [32].

With CMB and BAO data, we have constrained the parameter space of the spatially flat  $\Lambda$ CDM, scaling-DE, and spike-DE models that are favored by the observations. We limit our investigation by considering a spike-DE model with a dark energy spike occurring near the radiation-matter equality era ( $\log_{10} a_c = -3.5$ ); see Fig. 1. The reason for choosing such an epoch is that the transient domination of dark energy near the radiation-

TABLE II: Mean and standard deviation (68.3% confidence limit) of the conventional cosmological parameters estimated from the marginalized one-dimensional likelihood distribution for best-fit  $\Lambda$ CDM, scaling-DE, spike-DE models constrained with the Planck CMB and BAO data sets. For the tensor-to-scalar ratio  $r$  and the level of early dark energy  $B$ , the upper limits are presented.

Parameter	$\Lambda$ CDM	Scaling-DE	Spike-DE
$100\Omega_{b0}$	$4.784 \pm 0.076$	$4.870 \pm 0.102$	$4.727 \pm 0.026$
$\Omega_{c0}$	$0.2547 \pm 0.0081$	$0.2564 \pm 0.0084$	$0.2518 \pm 0.0031$
$h$	$0.6807 \pm 0.0069$	$0.6761 \pm 0.0077$	$0.6836 \pm 0.0037$
$\tau$	$0.090 \pm 0.012$	$0.093 \pm 0.013$	$0.086 \pm 0.011$
$n_s$	$0.9644 \pm 0.0056$	$0.9675 \pm 0.0061$	$0.9635 \pm 0.0046$
$r$	$< 0.054$	$< 0.061$	$< 0.048$
$\ln[10^{10} A_s]$	$3.084 \pm 0.022$	$3.088 \pm 0.024$	$3.081 \pm 0.021$
$t_0$ (Gyr)	$13.795 \pm 0.036$	$13.858 \pm 0.060$	$13.781 \pm 0.033$
$B$	...	$< 0.0022$	...

matter equality most affects the evolution of density perturbations in the scalar-field-based early dark energy model, inducing a highly oscillatory feature in the angular power spectrum of temperature fluctuations at high multipoles (see Fig. 3 of Ref. [22]). The free conventional cosmological parameters are  $\Omega_{b0}h^2$ ,  $\Omega_{c0}h^2$ ,  $h$ ,  $\tau$ ,  $n_s$ ,  $r$ , and  $\ln[10^{10} A_s]$ , where  $\Omega_{b0}$  ( $\Omega_{c0}$ ) is the baryon (CDM) density parameter at the current epoch,  $h$  is the normalized Hubble constant with  $H_0 = 100h \text{ km s}^{-1} \text{ Mpc}^{-1}$ ,  $\tau$  is the reionization optical depth,  $n_s$  is the spectral index of the primordial scalar-type perturbation,  $r$  is the ratio of tensor- to scalar-type perturbations, and  $A_s$  is the amplitude of the primordial curvature perturbations with  $A_s = k^3 P_{\mathcal{R}}(k)/(2\pi^2)$  at the pivot scale  $k_0 = 0.05 \text{ Mpc}^{-1}$ . The running of spectral index is not considered. There are also several foreground and calibration parameters (see Table I and [2] for detailed descriptions of the parameters).

The free parameters of spike-DE model are  $A$ ,  $B$ , and  $\sigma$  with  $a_c$  fixed [see Eq. (1)]. With conventional and dark energy model parameters all freely varying, the Markov chain Monte Carlo (MCMC) chains are not easily converged due to multiple local maxima in the multidimensional likelihood distribution. In this work, instead of obtaining the full converged MCMC chains for all the free parameters, we search for the best-fit location in the likelihood distribution by manually running the CosmoMC with an option `action=2` starting at the local maxima found from the trial MCMC chains obtained with all parameters varying. The results are summarized in Table I, which lists the parameters of  $\Lambda$ CDM, scaling-DE, and spike-DE models that best describe the observational data, together with the cosmic age ( $t_0$ ) and the parameters related with foregrounds and instrumental calibrations.

To see how the conventional cosmological parameters

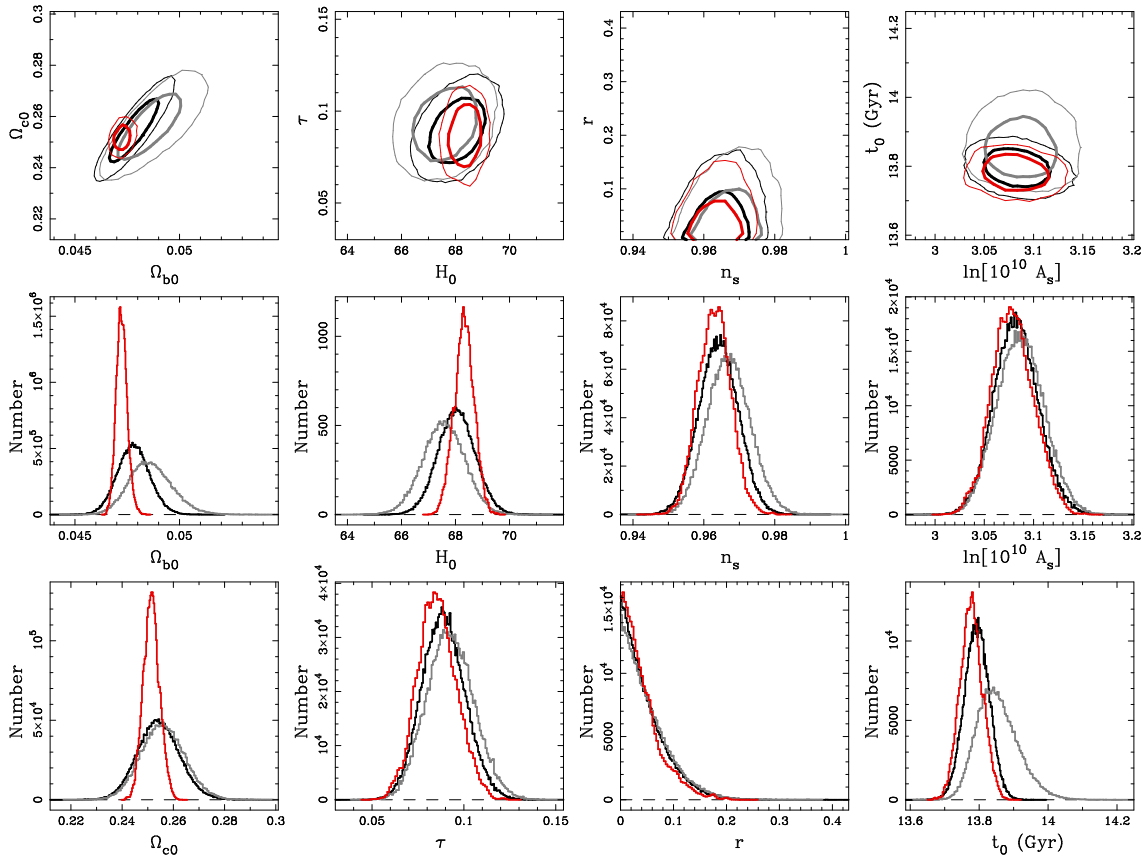


FIG. 2: Top: Two-dimensional likelihood contours of the conventional cosmological parameters favored by the Planck CMB and BAO data sets for spike-DE (red), scaling-DE (grey), and  $\Lambda$ CDM (black curves) models. For the spike-DE model, dark energy parameters have been fixed with the values given in Table I. The thick and thin solid curves indicate the 68.3% and 95.4% confidence limits, respectively. Middle and bottom: Marginalized one-dimensional likelihood distributions for each cosmological parameter, with arbitrary normalizations.

are affected by the presence of the dark energy spike, we apply the MCMC method to randomly explore the parameter space that is favored by observations. For the spike-DE model, we have fixed dark energy parameters  $A$ ,  $B$ , and  $\sigma$  with the best-fit values given in Table I. For the scaling-DE model, however, the parameter  $B$ , the initial level of early dark energy, has been freely varied. Figure 2 shows two-dimensional likelihood contours and marginalized one-dimensional likelihood distributions of conventional cosmological parameters favored by the Planck CMB and BAO data sets for the spike-DE, scaling-DE, and  $\Lambda$ CDM models, estimated from the converged MCMC chains. Note that here we present the likelihood distributions of  $\Omega_{b0}$  and  $\Omega_{c0}$  instead of  $\Omega_{b0}h^2$  and  $\Omega_{c0}h^2$ . Table II summarizes the mean and 68.3% confidence limit of cosmological parameters estimated from the one-dimensional likelihood distributions. For the tensor-to-scalar ratio  $r$  and the level of early dark energy  $B$ , the upper limits (68.3%) are given. Interestingly, compared with  $\Lambda$ CDM model, the spike-DE model gives narrower parameter constraints on baryon, CDM density parameters and Hubble constant with the standard deviations smaller by a factor of 2.9, 2.6, 1.9, respec-

tively, and best-fit values slightly deviating from those of  $\Lambda$ CDM model. Since the likelihoods of the spike-DE model sufficiently overlap with the  $\Lambda$ CDM ones, the estimated parameters of both models are still consistent with each other.

For the scaling-DE model, the parameter constraints are consistent with those of  $\Lambda$ CDM model, except for slightly larger values of baryon density and cosmic age. In this model we have set  $B$  as a free parameter to constrain the level of early dark energy density ( $\Omega_e = B$ ). The allowed range for the early dark energy is  $\Omega_e < 0.0045$  (95.4% confidence limit), which is narrower than the Planck constraint on the fluid-based early dark energy density parameter of Doran & Robbers [33] ( $\Omega_e < 0.009$ ; [2]). Recently, a substantial improvement on the constraint  $\Omega_e < 0.0036$  (at 95% confidence level) has been obtained by the Planck 2015 data analysis [34].

#### IV. MODEL COMPARISON

In this section, we compare the best-fit  $\Lambda$ CDM, scaling-DE, spike-DE models to see which model is preferred



TABLE III: Chi-square ( $\chi^2$ ) values of best-fit  $\Lambda$ CDM, scaling-DE, and spike-DE models, together with differences of chi-square ( $\Delta\chi^2$ ), Akaike information criterion ( $\Delta\text{AIC}$ ), and Bayesian information criterion ( $\Delta\text{BIC}$ ) relative to  $\Lambda$ CDM value, and  $p$ -values estimated from the likelihood ratio test (LRT) statistic.

Data	$\Lambda$ CDM	Scaling-DE	Spike-DE
Lowlike	2014.578	2014.178	2014.092
Commander	-7.304	-7.471	-8.096
CamSpec	7795.773	7796.223	7777.669
Lensing	9.892	9.190	9.881
DR7	0.858	0.620	0.439
DR9	0.431	0.603	0.812
6dF	0.019	0.034	0.036
Wiggle Z	0.047	0.024	0.021
Total $\chi^2$	9814.295	9813.400	9794.753
$\Delta\chi^2$	...	-0.895	-19.542
$p$ -value (LRT)	...	0.3441	$6.148 \times 10^{-4}$
$\Delta\text{AIC}$	...	1.105	-11.542
$\Delta\text{BIC}$	...	6.982	11.968

over the other by the current observations based on the statistical criteria such as the likelihood ratio test and the Akaike and Bayesian information criteria that are widely used in the model selection.

Table III lists the separate chi-square ( $\chi^2$ ) values for each likelihood data set used in the parameter estimation for the best-fit  $\Lambda$ CDM, scaling-DE, and spike-DE models (see Table I for the best-fit values). The negative chi-square values for **Commander** likelihood data appear due to the arbitrary normalization of log-likelihood in the CosmoMC software [38]. We note that the best-fit cosmological parameters in the presence of a dark energy spike near the radiation-matter equality gives a far smaller chi-square value than those of the  $\Lambda$ CDM model by about five times the number of new free parameters of the spike-DE model ( $A, B, \log_{10} a_c, \sigma$ ) with a difference  $\Delta\chi^2 \equiv \chi^2 - \chi^2_{\Lambda\text{CDM}} = -19.542$ , which is a significant improvement of data-fitting.

The three dark energy models considered here are nested in the sense that the  $\Lambda$ CDM and scaling-DE models are special cases of the spike-DE model. In this case, we can apply the likelihood ratio test (LRT) as a model selection method, where the null model is the  $\Lambda$ CDM model and the alternative model is the scaling-DE or spike-DE model [4, 12]. The test statistics is defined as the twice the natural logarithm of the ratio of likelihoods of the null and alternative hypotheses (models) and is equivalent to a difference of chi-square relative to the  $\Lambda$ CDM one,

$$Q = 2 \ln \frac{\mathcal{L}(H_{\Lambda\text{CDM}}|D)}{\mathcal{L}(H|D)} = \Delta\chi^2, \quad (7)$$

where  $\mathcal{L}(H|D)$  indicates the maximum likelihood of the alternative model ( $H$ ) given the data ( $D$ ), and likewise for the null model ( $H_{\Lambda\text{CDM}}$ ). The LRT statistic is a computationally cheap version of the Bayes factor which provides a criterion for penalizing models with more parameters based on the Bayesian theory [10]. The test statistic  $Q$  can be approximated as the  $\chi^2$ -distribution with degrees of freedom ( $df$ ) defined as the additional number of parameters of the nesting model ( $df = 4$  for spike-DE model, and  $df = 1$  for scaling-DE model). The  $p$ -value, the probability that the null hypothesis is supported by the observational data over the alternative one, is calculated from the cumulative  $\chi^2$ -distribution and presented in Table III. We find that the  $p$ -value for the spike-DE model as alternative is quite small ( $p = 6.1 \times 10^{-4}$ ), suggesting a strong preference to the spike-DE model against the  $\Lambda$ CDM model.

The Akaike information criterion (AIC) is defined as [5, 7, 12]

$$\text{AIC} = -2 \ln \mathcal{L} + 2k, \quad (8)$$

where  $k$  is the number of free parameters of the model considered. If the alternative model gives a smaller AIC compared with the null ( $\Lambda$ CDM) model, it is ranked as a better model because the discrepancy with the true model is considered to be smaller. It is generally accepted that the AIC difference of 5 or more gives a strong evidence supporting the model with smaller AIC value (see [8] for the reliability of the AIC method in cosmological model selection). The differences of AIC relative to the  $\Lambda$ CDM model ( $\Delta\text{AIC} = \Delta\chi^2 + 2df$ ) are listed in Table III. The scaling-DE model has a positive value of  $\Delta\text{AIC} = 1.1$ , which means that introducing the scaling dark energy without a spike into the  $\Lambda$ CDM model does not improve the fit much. On the other hand, the negative value of  $\Delta\text{AIC} = -11.5$  for the spike-DE model suggests that the alternative model of dark energy with early scaling behavior and a dark energy spike (near the radiation-matter equality) is strongly favored by the current cosmological observations over the  $\Lambda$ CDM model.

As an alternative to the AIC, the Bayesian information criterion (BIC) is often used for model selection, which assigns a conservative penalty for large sample size. The BIC is defined as [6, 7, 12]

$$\text{BIC} = -2 \ln \mathcal{L} + k \ln N, \quad (9)$$

where  $N$  is the number of data points. We set  $N = 2637$  for Planck+BAO data sets ( $31 \times 4 + 48 + 2451 + 8 + 6$  for Lowlike [TT, TE, EE, BB], Commander, CamSpec, lensing, and BAO data, respectively) to calculate the difference of BIC relative to the  $\Lambda$ CDM value ( $\Delta\text{BIC} = \Delta\chi^2 + df \ln N$ ), which are listed in Table III. Contrary to the AIC result, the spike-DE model has a positive value of  $\Delta\text{BIC} = 12.0$ . The strong evidence supporting the presence of dark energy spike by the AIC has disappeared, since the BIC penalizes complex models by the large number of data points as in the CMB observation.

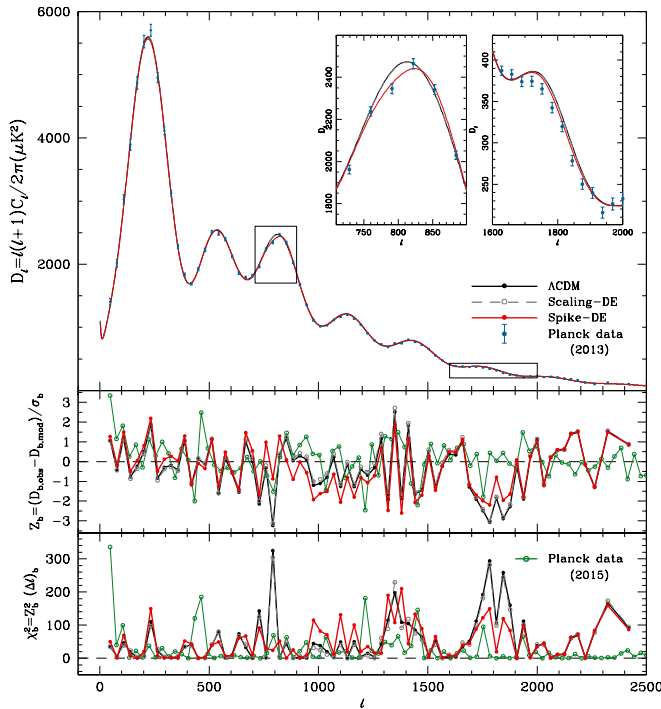


FIG. 3: Top: The CMB temperature angular power spectra of the best-fit  $\Lambda$ CDM (black), scaling-DE (grey), and spike-DE models (red curves). The angular power spectrum is given as  $D_\ell = \ell(\ell + 1)C_\ell / (2\pi)$  in  $\mu\text{K}^2$  unit. The Planck 2013 data points are shown with blue dots with error bars. Small panels inside magnify regions of  $\ell \approx 800$  and 1800. Middle and Bottom: the difference between observation and best-fit model prediction of band power divided by the measurement error ( $\sigma_b$ ) for each  $\ell$ -bin (denoted as  $b$ ),  $Z_b = (D_{b,\text{obs}} - D_{b,\text{mod}}) / \sigma_b$ , and the sum of contribution due to  $Z_b^2$  within the bin,  $\chi_b^2 = Z_b^2(\Delta\ell)_b$ . For comparison, the quantities  $Z_b$  and  $\chi_b^2$  estimated from the Planck 2015 data and the best-fit  $\Lambda$ CDM model prediction (constrained with Planck 2015 TT+LowP+Lesing data) are presented (green open circles; [3]).

In the context of BIC, the scaling-DE model with  $df = 1$  is preferred over the spike-DE model ( $df = 4$ ).

In summary, comparison of the maximum likelihoods of spike-DE and  $\Lambda$ CDM models according to LRT and AIC suggests that the spike-DE model is strongly preferred over the  $\Lambda$ CDM one while the BIC still indicates the observational data supports the simple  $\Lambda$ CDM model over others. From the definition of AIC and BIC we see that the AIC is inclined to select the model that better fits to the data while the BIC selects a simpler model with less parameters. Apart from the model selection between  $\Lambda$ CDM and spike-DE models, at least we conclude that the spike-DE model fits the observational data far better than  $\Lambda$ CDM model with the different cosmological parameter estimation.

According to Table III, the spike-DE model improves fitting to the CamSpec high  $\ell$  temperature likelihood data. Figure 3 verifies that the chi-square decrease is mainly

due to the better fitting of Planck temperature power spectrum data around the third ( $\ell \approx 800$ ) and sixth ( $\ell \approx 1800$ ) acoustic peaks where strong residuals relative to the best-fit  $\Lambda$ CDM model are seen. In the middle and bottom panels of Fig. 3, we plot the difference of the observed and the model-predicted band power spectra ( $D_b$ ) normalized with the measurement error ( $\sigma_b$ ) for each  $\ell$ -bin (here denoted as  $b$ ),  $Z_b = (D_{b,\text{obs}} - D_{b,\text{mod}}) / \sigma_b$ , and the sum of contribution due to  $Z_b^2$  within the bin,  $\chi_b^2 \equiv Z_b^2(\Delta\ell)_b$ , which approximates the chi-square contribution for each bin. The model band power  $D_{b,\text{mod}}$  is the average of the CMB angular power spectrum  $D_\ell = \ell(\ell + 1)C_\ell / (2\pi)$  predicted by a model within a specified bin. We use the same  $\ell$ -bins used in the Planck team's analysis. It was originally reported that the strong residuals seen around the third ( $\ell \approx 800$ ) and fifth ( $\ell \approx 1300$ –1500) acoustic peaks are real features of the primordial CMB sky [2]. We note that the best-fit spike-DE model significantly alleviates the strong residuals around the third ( $\ell \approx 800$ ) and sixth ( $\ell \approx 1800$ ) acoustic peaks observed in the best-fit  $\Lambda$ CDM model (red and black dots). However, the residual around the fifth peak ( $\ell \approx 1300$ –1500) still remains in both models.

## V. DISCUSSION AND CONCLUSION

In this paper, we investigate the observational effect of the early episodically dominating dark energy which accommodates a dark energy spike, a sudden transient variation in dark energy density, together with early scaling behaviors and late-time acceleration.

The dark energy model with a spike (spike-DE model) near the radiation-matter equality era improves the fit to the Planck CMB temperature power spectrum data around the third ( $\ell \approx 800$ ) and sixth ( $\ell \approx 1800$ ) acoustic peaks. Comparing the likelihood distributions based on the maximum likelihood ratio test and the Akaike information criterion as the statistical model selection methods, we find that the spike-DE model is strongly favored by observations over the conventional  $\Lambda$ CDM model. Furthermore, the spike-DE model provides the different cosmological parameter estimation with tighter constraints on matter density and Hubble constant (see Fig. 2 and Table II). However, the strong evidence supporting the presence of the dark energy spike disappears based on the Bayesian information criterion which assigns a conservative penalty to the model with a large number of parameters.

We have checked that including high- $\ell$  CMB data observed by the South Pole Telescope and the Atacama Cosmology Telescope [35, 36] or excluding the tensor-type perturbation do not affect our main results. Besides, we infer that the foreground and instrumental calibration parameters do not play a major role in improving the fit to the data. If they do, a significant reduction of chi-square should be seen in the case of  $\Lambda$ CDM model, too.

Very recently, the Planck 2015 data have been pub-

licly available. The main scientific conclusions of Planck 2015 data analysis are consistent with the previous results, with cosmological parameters deviating less than  $0.7\sigma$  [3]. As shown in Fig. 3, the strong residuals around  $\ell \approx 800$  and  $\ell \approx 1800$  in the Planck 2013 temperature power spectrum data are not observed in the Planck 2015 data; the deviation from the best-fit  $\Lambda$ CDM model prediction becomes quite smaller (see green open circles in the middle and bottom panels of Fig. 3). Therefore, the success of the spike-DE model in improving the fit to the Planck 2013 temperature power spectrum at those regions is not expected any more in the recent Planck 2015 data. However, the presence of strong residuals at  $\ell = 400$ – $500$  and  $\ell \approx 1200$  in the Planck 2015 data still leaves open the possibility that the new data are fitted by another candidate model of dark energy far better than  $\Lambda$ CDM model.

Through an example of the dark energy spike model, we emphasize that the alternative cosmological parameter estimation is allowed in the Einstein's gravity, with even better fitting of the same observational data than the conventional  $\Lambda$ CDM model.

## Acknowledgments

The author would like to thank Professor Jai-chan Hwang for valuable discussions. C.G.P. was supported by Basic Science Research Program through the National Research Foundation of Korea (NRF) funded by the Ministry of Science, ICT and Future Planning (No. 2013R1A1A1011107).

- 
- [1] G. Hinshaw *et al.* [WMAP Collaboration], *Astrophys. J. Suppl.* **208**, 19 (2013) [arXiv:1212.5226 [astro-ph.CO]].
  - [2] P.A.R. Ade *et al.* [Planck Collaboration], *Astron. Astrophys.* **571**, A16 (2014) [arXiv:1303.5076 [astro-ph.CO]].
  - [3] P.A.R. Ade *et al.* [Planck Collaboration], arXiv:1502.01589 [astro-ph.CO].
  - [4] J. Neyman and E.S. Pearson, *Royal Society of London Philosophical Transactions Series A* **231**, 289 (1933); S.S. Wilks, *Ann. Math. Stat.* **9**, 60 (1938).
  - [5] H. Akaike, *IEEE Transactions on Automatic Control* **19**, 716 (1974).
  - [6] G. Schwarz, *Ann. Stat.* **6**, 461 (1974).
  - [7] A.R. Liddle, *Mon. Not. R. Astron. Soc.* **351**, L49 (2004).
  - [8] M.Y.J. Tan, and R. Biswas, *Mon. Not. R. Astron. Soc.* **419**, 3292 (2012).
  - [9] A.F. Heavens, T.D. Kitching and L. Verde, *Mon. Not. Roy. Astron. Soc.* **380**, 1029 (2007) [astro-ph/0703191].
  - [10] T.D. Saini, J. Weller and S.L. Bridle, *Mon. Not. Roy. Astron. Soc.* **348** (2004) 603 [astro-ph/0305526].
  - [11] G. Efstathiou, *Mon. Not. Roy. Astron. Soc.* **388**, 1314 (2008) [arXiv:0802.3185 [astro-ph]].
  - [12] M. Szydlowski, A. Krawiec, A. Kurek, and M. Kamionka, *Eur. Phys. J. C* **75**, 5 (2015).
  - [13] A.R. Liddle, P. Mukherjee, D. Parkinson, and Y. Wang, *Phys. Rev. D* **74**, 123506 (2006).
  - [14] M.C. March, G.D. Starkman, R. Trotta and P.M. Vaudrevange, *Mon. Not. Roy. Astron. Soc.* **410**, 2488 (2011) [arXiv:1005.3655 [astro-ph.CO]].
  - [15] P. Serra, A. Heavens and A. Melchiorri, *Mon. Not. Roy. Astron. Soc.* **379**, 169 (2007) [astro-ph/0701338].
  - [16] M. Biesiada, B. Malec, and A. Piorkowska, *Research in Astronomy and Astrophysics*, **11**, 641 (2011).
  - [17] A. Borowiec, W. Godlowski and M. Szydlowski, *eConf C 0602061* (2006) 09 [Int. J. Geom. Meth. Mod. Phys. **4** (2007) 183] [astro-ph/0607639].
  - [18] A. De Felice, S. Nesseris, and S. Tsujikawa, *J. Cosmol. Astropart. Phys.* **5**, 029 (2012).
  - [19] S. del Campo, J.C. Fabris, R. Herrera and W. Zimdahl, *Phys. Rev. D* **83** (2011) 123006 [arXiv:1103.3441 [astro-ph.CO]].
  - [20] Y. Gong, X.-m. Zhu and Z.H. Zhu, *Mon. Not. Roy. Astron. Soc.* **415**, 1943 (2011) [arXiv:1008.5010 [astro-ph.CO]].
  - [21] J. Lu, L. Xu, J. Li, B. Chang, Y. Gui and H. Liu, *Phys. Lett. B* **662**, 87 (2008) [arXiv:1004.3364 [astro-ph.CO]].
  - [22] C.-G. Park, J.-h. Lee, J.-c. Hwang, & H. Noh, *Phys. Rev. D* **90**, 083526 (2014).
  - [23] A. Lewis and A. Lasenby, *Astrophys. J.* **513**, 1 (1999); A. Lewis, A. Challinor, and A. Lasenby, *Astrophys. J.* **538**, 473 (2000).
  - [24] A. Lewis, and S. Bridle, *Phys. Rev. D* **66**, 103511 (2002).
  - [25] W. Hu and I. Sawicki, *Phys. Rev. D* **76**, 104043 (2007) [arXiv:0708.1190 [astro-ph]]; W. Hu, *Phys. Rev. D* **77**, 103524 (2008) [arXiv:0801.2433 [astro-ph]]; W. Fang, S. Wang, W. Hu, Z. Haiman, L. Hui and M. May, *Phys. Rev. D* **78**, 103509 (2008) [arXiv:0808.2208 [astro-ph]]; W. Fang, W. Hu and A. Lewis, *Phys. Rev. D* **78**, 087303 (2008) [arXiv:0808.3125 [astro-ph]].
  - [26] G. Hinshaw, D. Larson, E. Komatsu *et al.* *Astrophys. J. Suppl.* **208**, 19 (2013).
  - [27] P.A.R. Ade *et al.* [Planck Collaboration], *Astron. Astrophys.* **571** (2014) A15 [arXiv:1303.5075 [astro-ph.CO]].
  - [28] P.A.R. Ade *et al.* [Planck Collaboration], *Astron. Astrophys.* **571** (2014) A17 [arXiv:1303.5077 [astro-ph.CO]].
  - [29] N. Padmanabhan, X. Xu, D.J. Eisenstein, R. Scalzo, A.J. Cuesta, K.T. Mehta and E. Kazin, *Mon. Not. Roy. Astron. Soc.* **427**, 2132 (2012) [arXiv:1202.0090 [astro-ph.CO]].
  - [30] F. Beutler, C. Blake, M. Colless, D.H. Jones, L. Staveley-Smith, L. Campbell, Q. Parker and W. Saunders *et al.* *Mon. Not. Roy. Astron. Soc.* **416**, 3017 (2011) [arXiv:1106.3366 [astro-ph.CO]].
  - [31] L. Anderson, E. Aubourg, S. Bailey, D. Bizyaev, M. Blanton, A.S. Bolton, J. Brinkmann and J.R. Brownstein *et al.*, *Mon. Not. Roy. Astron. Soc.* **427**, 3435 (2013) [arXiv:1203.6594 [astro-ph.CO]].
  - [32] C. Blake, S. Brough, M. Colless, C. Contreras, W. Couch, S. Croom, D. Croton and T. Davis *et al.* *Mon. Not. Roy. Astron. Soc.* **425**, 405 (2012) [arXiv:1204.3674 [astro-ph.CO]].
  - [33] M. Doran and G. Robbers, *J. Cosmol. Astropart. Phys.* **06**, 026 (2006).



- [34] P.A.R. Ade *et al.* [Planck Collaboration], arXiv:1502.01590 [astro-ph.CO].
- [35] R. Keisler, C.L. Reichardt, K.A. Aird, B.A. Benson, L.E. Bleem, J.E. Carlstrom, C.L. Chang and H.M. Cho *et al.*, *Astrophys. J.* **743**, 28 (2011).
- [36] S. Das, T. Louis, M.R. Nolta, G.E. Addison, E.S. Battistelli, J.R. Bond, E. Calabrese and D.C.M.J. Devlin *et al.*, *JCAP* **1404**, 014 (2014) [arXiv:1301.1037 [astro-ph.CO]].
- [37] An ESA science mission with instruments and contributions directly funded by ESA Member States, NASA, and Canada; <http://www.esa.int/Planck>
- [38] <http://cosmocoffee.info/viewtopic.php?t=2216>